Shear Viscosity of Strongly Coupled Yukawa Systems on Finite Length Scales

K. Y. Sanbonmatsu and M. S. Murillo

Los Alamos National Laboratory, Los Alamos, New Mexico 87545
(Received 21 July 2000; revised manuscript received 17 October 2000)

The Yukawa shear viscosity has been calculated using nonequilibrium molecular dynamics. Near the viscosity minimum, we find exponential decay consistent with the Navier-Stokes equation, with significant deviations on finite length scales for larger viscosity values. The viscosity is determined to be nonlocal on a scale length consistent with the correlation length, revealing the length scales necessary for obtaining transport coefficients in the hydrodynamic limit by nonequilibrium molecular dynamics methods. Our results are quasiuniversal with respect to excess entropy for excess entropies well below unity.

A broad variety of systems, including dusty plasmas, inertial confinement fusion dense plasmas, brown dwarfs, giant planets, white dwarfs, and neutron stars, may be modeled as strongly coupled Coulomb systems. Often one is concerned with the dynamics of the heaviest species—whether it be dust grains or ions—which are screened by the lighter particles. A general unifying model for all of these systems is the Yukawa model, whose interparticle pair potential is of the form $u_Y(r)/T = \Gamma \exp(-\kappa r/a)/(r/a)$, where $\Gamma = Q^2/(aT)$ and $\kappa = a/\lambda_D$, defined in terms of the charge Q, temperature T, half the interparticle spacing a, and screening length λ_D. In fact, recent measurements [1] have shown the intergrain potential in dusty plasmas to be closely of the Yukawa form. Dense $(n > 10^{20}$ cm$^{-3})$ plasmas can be modeled as Yukawa systems [2], which in turn have numerous astrophysical applications [3]. The Yukawa system will likely emerge as a useful model for the recently produced ultracold neutral plasmas [4].

The shear viscosity is a dynamic property essential for predicting collective mode properties of strongly coupled plasmas, an issue at the forefront of the rapidly evolving field of dusty plasma physics [5,6]. The viscosity is also important for determining Rayleigh-Taylor instability growth rates in inertial confinement fusion targets [7] and, in general, the damping of waves in dense plasmas [8]. In some cases, such as dusty plasmas and ultracold plasmas, viscous damping competes with damping due to background neutrals. However, typical dusty plasma experiments can probe regimes where the shear viscosity dominates.

The viscosity of the one-component plasma (OCP), i.e., the $\kappa = 0$ case of the Yukawa model, has been known for over two decades [9]. The dependence of the viscosity on Γ was shown for the OCP in the seminal paper by Vieille-fosse and Hansen [9] and later confirmed [10,11]. Despite the wide applicability of the Yukawa model, the effect of finite κ is unknown. Approximate methods based on excess entropy appear promising for providing estimates [12–14]. Moreover, little is known about the viscosity on finite length scales, where the viscosity is nonlocal, for either the OCP or Yukawa models [6,15].

Because of the difficulties with long time tails of the current autocorrelation function in equilibrium calculations of the shear viscosity [9], several nonequilibrium molecular dynamics (NEMD) techniques have been devised for hard sphere and Lennard-Jones systems which prove much faster than equilibrium methods [16]. We employ the NEMD method introduced previously by Donko and Nyiri for the OCP [11], which is a method well suited to study finite length effects. We performed parallel NEMD simulations by imposing a sinusoidal shear velocity profile and measuring the decay time. We implemented minimum image molecular dynamics in parallel on an 8 CPU LINUX cluster using a simple replicated data parallelization scheme. The system was equilibrated for $10-100\tau_{ac}$ (the autocorrelation time τ_{ac} is defined by the e-folding time of the velocity autocorrelation function) using velocity scaling. The time step was chosen to ensure energy conservation within 5% in the absence of velocity scaling. The scale length of the shear profile was varied by using $N = 3200$, 6400, $12\,800$, and $25\,600$ particles. With the box size $L = 23.75a$, the force for $\kappa = 1$ on a particle due another particle one box length away was smaller by $\approx 10^{-5}$ compared with neighboring particles, justifying our neglecting Ewald sums. This was verified by performing a simulation for $\kappa = 1$ and $\Gamma = 1000$ including the forces due to 26 neighboring image simulation boxes. After equilibration, a sinusoidal velocity profile was applied and the velocity scaling was turned off. At $t = 0$, the transverse velocity profile has the form

$$\mathbf{v}_i(0) = v_z(0)\sin(qx_i)\hat{\mathbf{z}} + \mathbf{v}_{i,\text{therm}}, \qquad (1)$$

where $\mathbf{v}_{i,\text{therm}}$ is the initial random thermal velocity of particle i and x_i its x coordinate. The velocity profile amplitude $v_z(t)$ of the system was obtained by a least squares fit of the simulation velocity profile to $v_z(t)\sin(qx)$. The decay time τ_s was then obtained by a least squares fit of $v_z(t)$ to $v_z(t) = v_z(0)\exp[-t/\tau_s(q)]$ between $t = 2\tau_{ac}$ and e-folding time $t = t_{max}$, where $v_z(t_{max}) = v_z(2\tau_{ac})/e$. This eliminated any short time correlations and ensured a long enough simulation time to obtain the exponential decay constant. The exponential decay

profile is the solution to the transverse part of the linear Navier-Stokes equation:

$$\frac{\partial v_z(\mathbf{r}, t)}{\partial t} = \frac{1}{Mn} \int d^3r' \, \eta(\mathbf{r} - \mathbf{r}') \nabla^2 v_z(\mathbf{r}', t), \quad (2)$$

for the initial condition (1). Nonlocality has been allowed for by introducing a convolution over the nonlocal viscosity $\eta(\mathbf{r} - \mathbf{r}')$. Here $\tau_s(q) = nM/q^2 \eta(q)$, where $q = 2\pi/L$. By varying the simulation size L the viscosity was obtained for various wave vectors. The initial velocity amplitude was $v_z(0) \approx 0.86 v_{th}$, where $v_{th} \equiv (T/M)^{1/2}$, corresponding to the perturbation $\delta T/T \approx 0.12$.

The viscosity was computed over the range $2 < \Gamma < 1000$ and $1 < \kappa < 4$. Our most accurate simulation results are displayed in Table I. Figure 1 displays the viscosity surface $\eta^*(\Gamma, \kappa)$ over the Γ-κ plane, where our simulation data (Table I) have been interpolated to the surface using a minimum curvature surface and $\eta^* \equiv \eta/(Mn\omega_p a^2)$. The values of η at $\kappa = 0$ and $\Gamma = 2, 5, 10, 100$ are taken from Donko and Nyiri [11]. In Fig. 2 the viscosity is shown versus Γ for $\kappa = 0, 1, 2, 3, 4$. Shown in the inset in Fig. 2 is η^* versus Γ for $\kappa = 1$ based on the NEMD results, the CP method of Murillo (CP1), and a new CP (CP2) method. The new CP method uses the excess entropy scaling of the viscosity [13,14], where the Yukawa excess entropy has been estimated from the known OCP excess entropy and the OCP-Yukawa correspondence [12].

Screening lowers the minimum in the viscosity from $\eta^* \approx 0.09$ at $\kappa = 0$ to $\eta^* < 0.02$ for $\kappa = 3$ and $\eta^* < 0.01$ for $\kappa = 4$ (Fig. 1). This significant decrease in the minimum is in direct contradiction with the CP estimates that predict the minimum viscosity of all Yukawa systems to be equal to the OCP minimum [12]. Screening also shifts the minimum viscosity, causing it to appear at larger Γ as κ is increased.

Figure 3 displays the reduced viscosity $\eta^+ = \eta^*\sqrt{3\Gamma} (3/4\pi)^{1/3}$ versus excess entropy s, where $s = -S/Nk_B$, and S is the actual excess entropy, N is the number of particles, and k_B is the Boltzmann constant. The excess entropy was computed using the molecular dynamics results of Hamaguchi *et al.* [17]. Rosenfeld has shown that transport coefficients are quasiuniversal on such a plot for excess entropies above $s = 1$ [13]. We have found the surprising result that quasiuniversality holds well below unity over the range $1 < \kappa < 4$. Also

shown are the OCP results of Vieillefosse and Hansen [9], Wallenborn and Baus [10], and Donko and Nyiri [11].

Figure 4 demonstrates that the viscosity is sometimes monotonic ($\Gamma = 100, 1000$) and sometimes not monotonic ($\Gamma = 2, 5, 10$) in κ for $0 < \kappa < 4$ depending on the strength of Γ. For $\Gamma = 2$, curves for both $N = 3200$ and $N = 25\,600$ are shown. For $\Gamma = 100$, the viscosity falls off with κ due to decreasing strong coupling correlation length r_{corr} (the length over which the radial distribution function's successive maxima fall off by $1/e$ beginning with the second maximum). The viscosity shows a minimum for $\Gamma = 10$ where the apparently large value of the mean free path λ_{mfp} determines the viscosity for $\kappa = 2$–4.

The Navier-Stokes equation breaks down in regimes of extreme weak coupling ($\Gamma = 2$) and regimes of extreme strong coupling ($\Gamma = 1000$). The breakdown results from the large λ_{mfp} for $\Gamma = 2$ and the large r_{corr} at $\Gamma = 1000$ causing large errors in η (Fig. 4). The error bars in Fig. 4 were determined by the dispersion in viscosity resulting from starting the exponential fit of the $v_z(t)$ decay curve (Fig. 5) at $t = 1, 2, 3, 4, 5\tau_{ac}$. This error was larger than fluctuations due to different initial conditions (only error bars larger than 5% are shown). Nonexponential decay is demonstrated in Fig. 5(a) ($\Gamma = 2$, $N = 3200$) for the case of $\kappa = 4$. A curve of similar nonexponential shape was also observed for $\kappa = 3$. We attribute the nonexponential decay to a transition to the Knudsen gas regime for which the Knudsen number $\mathcal{K}$, defined as $\mathcal{K} = \lambda_{mfp}/L$, exceeds unity (violating the condition of validity for the Navier-Stokes equation which requires $\lambda_{mfp} \ll L$). This was verified by decreasing the box length from $L = 23.75a$ to $L = 11.88a$ for $\kappa = 1, 2$, where we find that the decay changes from exponential to nonexponential (similar to the nonexponential shape observed for $\kappa = 3, 4$ and $L = 23.75a$) suggesting

TABLE I. Yukawa shear viscosity. * denotes simulations performed with $N = 25\,600$. All other values used $N = 3200$.

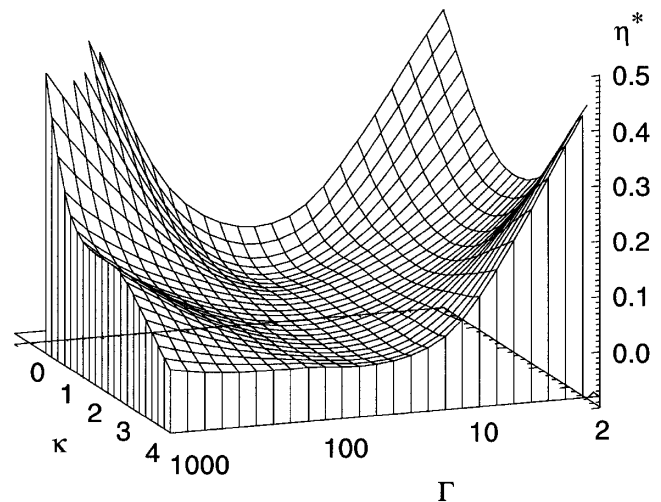| Γ	$\kappa = 1$	2	3	4
2	0.2340*	0.2646	0.4760*	0.5496*
5	0.0829*	0.0829*	0.1549	0.1633
10	0.0526*	0.0521	0.0693	0.0870
100	0.0568*	0.0224	0.0170	0.0142
1000	0.2191	0.1541	0.0351	0.0106

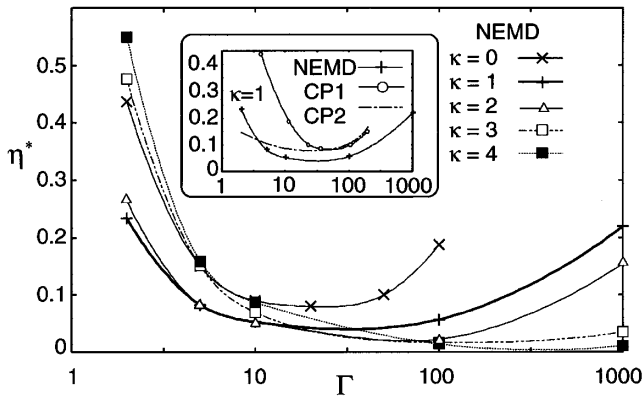FIG. 1. The Yukawa shear viscosity surface $\eta^*(\Gamma, \kappa)$ for the values in Table I.

FIG. 2.   The NEMD shear viscosity versus coupling parameter Γ for screening parameters $\kappa = 1, 2, 3, 4$ for the values in Table I. The $\kappa = 0$ case is taken from Donko and Nyiri. The inset compares NEMD and CP (described in text).

FIG. 4.   The viscosity $\eta^*(\kappa)$ for $\Gamma = 2, 5, 10, 100, 1000$ for the most accurate values in Table I with the exception of $\Gamma = 2$.

that we have located a transition to the regime where $L \approx \lambda_{\mathrm{mfp}}$. This effect was also confirmed for $\kappa = 3, 4$, where exponential decays were observed for large systems with $N = 25\,600$ and $L = 47.51a$. These points with $N = 25\,600$ are shown in Fig. 4, demonstrating that the decrease in η with respect to κ for $\kappa > 2$ and $N = 3200$ is due to the transition to the Knudsen gas. This indicates the minimum length scale for which the Navier-Stokes equation is applicable.

The opposite extreme ($\Gamma = 1000, \kappa = 1, 2$) is near the crystallization boundary [17], where viscoelastic behavior is expected to emerge. Furthermore, correlations in the radial distribution function $g(r)$ are observed out to $r \approx 10a \approx L/2$, making the validity of (2), which requires $r_{\mathrm{corr}} \ll L$, marginal. We therefore used the viscoelastic generalization of (2),

$$\left(1 + \tau \frac{\partial}{\partial t}\right) \frac{\partial v_z(\mathbf{r}, t)}{\partial t} = \frac{1}{Mn} \int d^3r' \, \eta(\mathbf{r} - \mathbf{r}') \\ \times \nabla^2 v_z(\mathbf{r}', t), \tag{3}$$

whose solution is of the form

$$v_z(t) = v_z(0)e^{-t/(2\tau)}\left[\cos(\omega_0 t) + \frac{1}{2\tau\omega_0}\sin(\omega_0 t)\right], \tag{4}$$

where $\omega_0 = (q^2\eta/\tau Mn - 1/4\tau^2)^{1/2}$. Based on simulation results at short times, the initial condition was taken to have $dv_z(0)/dt = 0$. As shown in Fig. 5(b), the viscoelastic solution (lighter dashed curve) is a significant improvement over the Navier-Stokes solution, giving $\tau = 44.55\omega_p^{-1}$, $\omega_0 = 0.0123\omega_p$, and $\eta^* = 0.177$, approximately 15% higher than the Navier-Stokes value with significantly smaller error. For $\Gamma = 1000$, $\kappa = 3, 4$, the decay is closer to exponential, consistent with the shorter correlation lengths $r_{\mathrm{corr}} \approx 5a$ observed in our simulations.
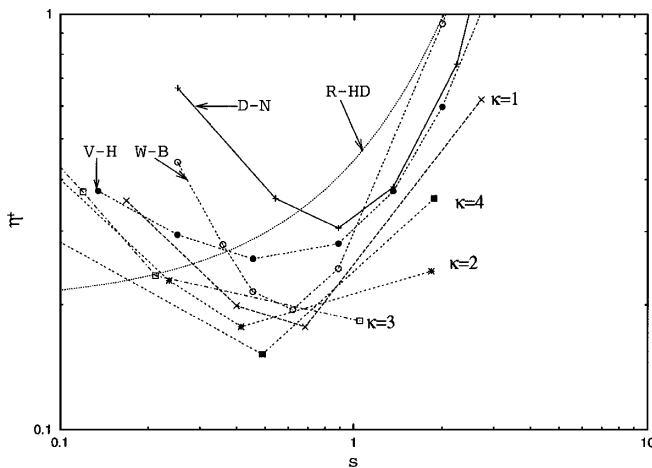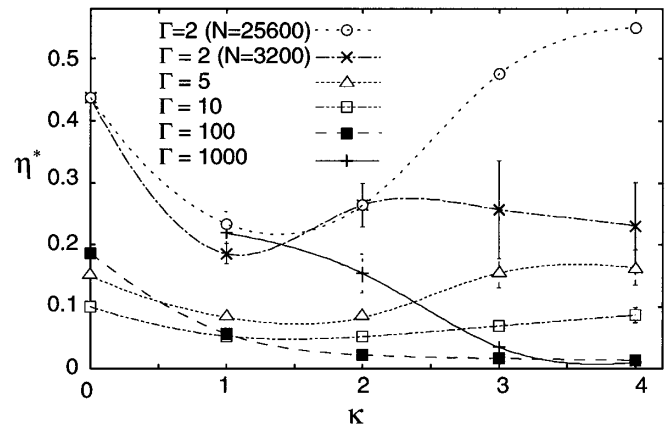

FIG. 3.   Reduced viscosity versus excess entropy for $\kappa = 1, 2, 3, 4$. Also shown are the OCP results of Vieillefosse and Hansen (V-H), Wallenborn and Baus (W-B), and Donko and Nyiri (D-N). The high density fit $\eta^+ = 0.2e^{0.8s}$ of Rosenfeld (R-HD) is also shown.
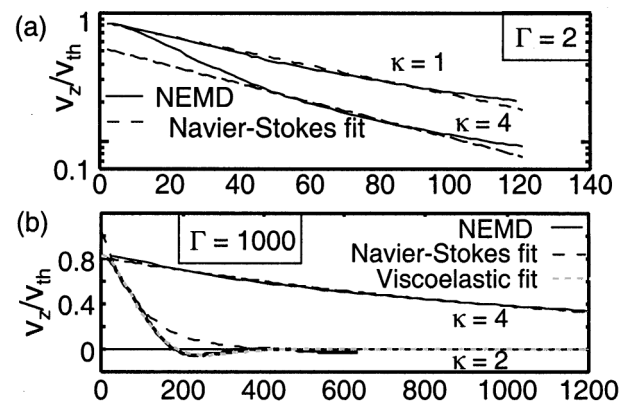

FIG. 5.   (a) The velocity profile decay amplitude for weak ($\kappa = 1$) and strong ($\kappa = 4$) screening at $\Gamma = 2$. Note the deviations from exponential decay. (b) The velocity profile decay amplitude for weak ($\kappa = 2$) and strong ($\kappa = 4$) screening at $\Gamma = 1000$.
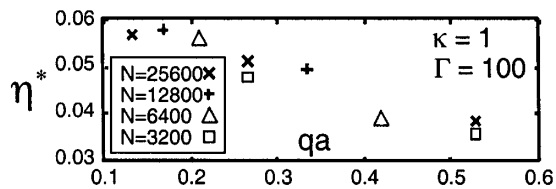
FIG. 6. Wave number dependence of the viscosity $\eta^*(q)$ for $\Gamma = 100$, $\kappa = 1$. The knee at $qa \approx 0.3$ is due to the increase in r_{corr}/L with q. For this case the hydrodynamic limit is obtained for $N = 6400$ particles and $qa \approx 0.21$.

The Navier-Stokes equation breaks down for smaller box sizes, i.e., larger q and smaller N, due to $\lambda_{\mathrm{mfp}} \approx L$ (weakly coupled) or $r_{\mathrm{corr}} \approx L$ (strongly coupled). This breakdown suggests nonlocal effects are important in determining the viscosity on these length scales. We have explored this phenomenon with simulations for the case $\Gamma = 100$ and $\kappa = 1$ for various numbers of particles from $N = 3200$ to $N = 25\,600$, as well as various values of n for $q = 2\pi n/L$. Figure 6 demonstrates that the viscosity is fairly constant for small q and decreases towards short wavelengths with the knee occurring near $q = 0.3$. This corresponds to a length scale where hydrodynamic generalizations are expected since $L \approx r_{\mathrm{corr}}$. We conjecture that this could be measured in a dusty plasma since the scale lengths ($\sim$mm) are macroscopic. We do not expect η to change substantially for lower q (i.e., $N \gg 25\,600$) since $L \gg r_{\mathrm{corr}}$ for $N = 25\,600$; that is, the simulation with $N = 25\,600$ is in the hydrodynamic limit. This could be tested by performing simulations with $N \gg 25\,600$ using the particle-particle/particle-mesh technique [18]. It is noted that standard particle-in-cell methods are impractical because accurate determination of viscosity requires accurate treatment of short-range interactions (i.e., $\ll 1$ particle per cell) where the simulation time is limited by the three-dimensional grid size rather than the number of particles [19]. We expect the viscosity to be slightly underestimated for values of κ and Γ where results were obtained only for $N = 3200$.

We have found that the decay of the velocity profile deviates from the usual Navier-Stokes exponential decay when the scale length becomes less than either the mean free path or the correlation length. Increasing the length scale (wavelength) under fixed conditions recovered the exponential decay and, therefore, the hydrodynamic limit. Under conditions of weak coupling we interpret the nonexponential decay as a transition to the Knudsen gas regime and, for strong coupling, as a transition to a strongly coupled liquid with nonlocal viscosity. Near the viscosity minimum for $\kappa = 1$ we have shown that the viscosity is scale-length dependent over a distance of approximately one correlation length. Near the phase boundary we have found that the decay resembles the solution to the viscoelastic generalization of the Navier-Stokes. For the longest wavelengths in our simulations we have fit the exponential decay to the solution of the Navier-Stokes solution and have obtained the shear viscosity. Our results indicate that the Yukawa shear viscosity is quasiuniversal with respect to excess entropy, even below $s = 1$ where the plasma is only moderately coupled and caging is not very strong.

[1] U. Konopka, G. E. Morfill, and L. Radtke, Phys. Rev. Lett. **84**, 891 (2000).
[2] Y. Rosenfeld, E. Nardi, and Z. Zinamon, Phys. Rev. Lett. **75**, 2490 (1995).
[3] S. Ichimaru, *Statistical Plasma Physics: Condensed Plasmas*, Frontiers in Physics Vol. 88 (Addison-Wesley, New York, 1994).
[4] S. Kulin, T. C. Killian, S. D. Bergeson, and S. L. Rolston, Phys. Rev. Lett. **85**, 318 (2000).
[5] P. K. Kaw and A. Sen, Phys. Plasmas **5**, 3552 (2000).
[6] M. S. Murillo, Phys. Rev. Lett. **85**, 2514 (2000).
[7] J. G. Clerouin, M. H. Cherfi, and G. Zerah, Europhys. Lett. **42**, 37 (1998).
[8] V. M. Atrazhev and I. T. Iakubov, Phys. Plasmas **2**, 2624 (1995).
[9] P. Vieillefosse and J. P. Hansen, Phys. Rev. A **12**, 1106 (1975).
[10] J. Wallenborn and M. Baus, Phys. Lett. **61A**, 35 (1977); Phys. Rev. A **18**, 1737 (1978); B. Bernu, P. Vieillefosse, and J.-P. Hansen, Phys. Lett. **63A**, 301 (1977).
[11] Z. Donko and B. Nyiri, Phys. Plasmas **7**, 45 (2000).
[12] M. S. Murillo, Phys. Rev. E **62**, 4115 (2000).
[13] Y. Rosenfeld, Phys. Rev. A **15**, 2545 (1977).
[14] Y. Rosenfeld, J. Phys. Condens. Matter **11**, 5415 (1999).
[15] M. Baus and J. Wallenborn, J. Stat. Phys. **16**, 91 (1977).
[16] E. M. Gosling, I. R. McDonald, and K. Singer, Mol. Phys. **26**, 1475 (1973).
[17] S. Hamaguchi, R. T. Farouki, and D. H. E. Dubin, Phys. Rev. E **56**, 4671 (1997).
[18] R. W. Hockney and J. W. Eastwood, *Computer Simulation Using Particles* (Adam Hilger, Cambridge, England, 1988).
[19] K. Y. Sanbonmatsu, L. E. Thode, H. X. Vu, and M. S. Murillo, J. Phys. IV (France) **10**, (2000).